Materials Research Letters

ISSN: (Print) 2166-3831 (Online) Journal homepage: https://www.tandfonline.com/loi/tmrl20

Grain Size Effect on Deformation Mechanisms of Nanocrystalline bcc Metals

G.M. Cheng, W.W. Jian, W.Z. Xu, H. Yuan, P.C. Millett & Y.T. Zhu

To cite this article: G.M. Cheng, W.W. Jian, W.Z. Xu, H. Yuan, P.C. Millett & Y.T. Zhu (2013) Grain Size Effect on Deformation Mechanisms of Nanocrystalline bcc Metals, Materials Research Letters, 1:1, 26-31, DOI: 10.1080/21663831.2012.739580

To link to this article: https://doi.org/10.1080/21663831.2012.739580

MATERIALS RESEARCH LETTERS

Mater. Res. Lett., 2013
Vol. 1, No. 1, 26–31, http://dx.doi.org/10.1080/21663831.2012.739580

Taylor & Francis
Taylor & Francis Group

www.tandfonline.com/toc//current

Grain Size Effect on Deformation Mechanisms of Nanocrystalline bcc Metals

G. M. Cheng[a], W. W. Jian[a], W. Z. Xu[a], H. Yuan[a], P. C. Millett[b] and Y. T. Zhu[a,*]

[a]*Department of Material Science and Engineering, North Carolina State University, Raleigh, NC 27695, USA;*
[b]*Fuels Modeling and Simulations, Idaho National Laboratory, Idaho Falls, ID 83415, USA*

(*Received 04 September 2012; final form 07 October 2012*)

Supplementary Material Available Online

Nanocrystalline (NC) body-centered cubic (bcc) metals behave very differently from how NC metals with other crystal structures behave. Their strain rate sensitivity decreases with decreasing grain size, which is an observation that has not been well understood. Here, we report a significant effect of grain size on the deformation mechanism of NC bcc Mo. With decreasing grain size, the density of mixed and edge dislocations increases, while the density of screw dislocations decreases. When the grains become very small, the overall dislocation density decreases with decreasing grain size. These observations provide a logical explanation for the observed effect of grain size on strain rate sensitivity.

Keywords: Dislocation, bcc, Nanocrystalline, Grain Size, Deformation Mechanism

A decade ago, it has been found that nanocrystalline (NC) body-centered cubic (bcc) metals have a much lower strain rate sensitivity than their coarse-grained counterparts [1–5]. This finding is significant and surprising because it is opposite to the findings in NC metals with face-centered cubic (fcc) and hexagonal close-packed (hcp) crystal structures [2,3,6]. There have been attempts to explain this unique mechanical behavior of bcc metals based on the slip of screw dislocations via the kink-pair nucleation mechanism observed in coarse-grained bcc metals. Assuming that the deformation mechanism remains the same in NC metals, it follows that a higher flow stress is responsible for the observed lower strain rate sensitivity with decreasing grain size [3]. This is based on the following equation:

$$m = k_{\mathrm{B}}T/\tau v^{*}, \tag{1}$$

where m is the strain rate sensitivity, k_{B} is the Boltzmann constant, T is the absolute temperature, τ is the applied shear stress and v^{*} is the activation volume [2,3]. With decreasing grain size, τ increases following the Hall–Petch relationship, while v^{*} levels off with increasing stress, which leads to decreasing strain rate sensitivity.

The above explanation on the effect of grain size on strain rate sensitivity, while logical, leads to some unanswered questions. First, the assumption that screw dislocations control the deformation behavior in NC bcc metals has not been experimentally verified. In addition, screw dislocations control the deformation behavior only in the early stage of deformation [2,6,7], suggesting that the controlling mechanism could change with the evolution of the microstructure. Indeed, it was reported that the strain rate sensitivity leveled off with increasing stress in bcc Fe in the stage IV deformation [8]. Second, it was observed that when the grain sizes become very small, the strain rate sensitivity appears to reach a minimum and then increase slightly when the grain size decreases further. This behavior has not been understood. These questions can only be answered by understanding the effect of grain size on the deformation mechanisms of NC bcc metals.

In this study, we found a significant effect of grain size on the densities of dislocations of various types in NC and ultrafine-grained bcc Mo, suggesting that the grain size affects the deformation mechanisms of bcc Mo. We chose Mo as a model bcc metal because it is not magnetic, which makes it easier to observe the dislocation structures using transmission electron microscopy (TEM). NC bcc Mo samples were produced by high-pressure torsion (HPT) [9,10] under a pressure of 4 GPa

*Corresponding author. yuntian.zhu@gmail.com, ytzhu@ncsu.edu

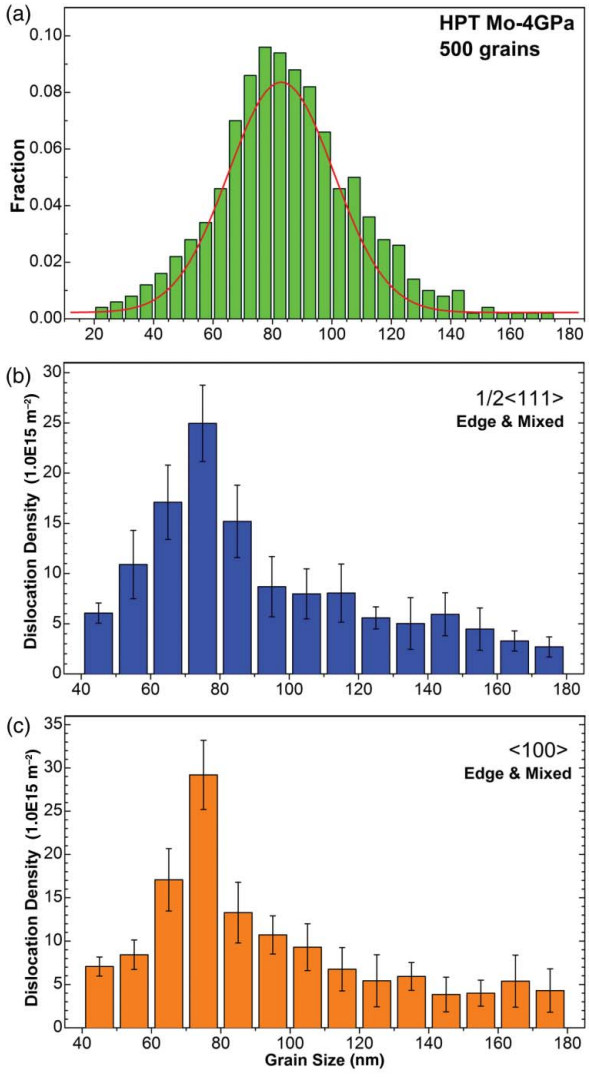

Figure 1. (a) The distribution of grain sizes of NC Mo based on 500 grains examined under TEM. The average grain size is ~85 nm. (b) The variation of the density of ½⟨111⟩ edge and mixed dislocations with decreasing grain size from a total of 86 grains. (c) The variation of the density of ⟨100⟩ edge and mixed dislocations with decreasing grain size from a total of 88 grains. The size of a grain was measured from TEM micrographs by approximating the two-dimensional grain image as an ellipsis and the size of the grains was calculated as $d = \sqrt{ab}$, where a and b are the short and long axes of the ellipse, respectively.

for six revolutions. In Figure 1, (a) the distribution of grain sizes of 500 grains examined under TEM, (b) the statistical variation of the density of edge and mixed ½⟨111⟩ dislocations with grain size and (c) the statistical variation of the density of edge and mixed ⟨100⟩ dislocations with grain size are shown. The dislocation density was calculated as the number of dislocations per unit area in high-resolution TEM (HRTEM) micrographs. The best zone axes in differentiating ½⟨111⟩ edge and mixed dislocations from ⟨100⟩ edge and mixed dislocations are the ⟨110⟩ zone axes. More detailed TEM image analyses will be published in another publication. The mixed

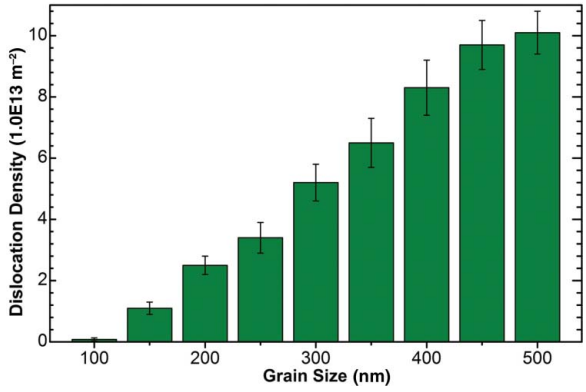

Figure 2. The effect of grain size on the density of screw dislocations, which was calculated as the total length of screw dislocation segments per unit volume.

dislocations are those whose Burgers vectors have both edge and screw components; that is, they are not pure edge or pure screw dislocations.

Figure 1(b) reveals that the density of the ½⟨111⟩ edge and mixed dislocations first increases and then decreases with decreasing grain size. The maximum density reached is 2.5×10^{16} m^{-2} at the grain size of ~75 nm. This is comparable to the dislocation density in heavily deformed fcc and hcp metals [11–13]. In the bcc crystal structure, ½⟨111⟩ are the Burgers vectors of the perfect dislocations, which are along the close-packed directions [14,15]. They are responsible for the deformation of most bcc metals and alloys. The observation of a high density of ½⟨111⟩ edge and mixed dislocations indicates that the edge and mixed dislocations contributed significantly to the deformation of NC Mo and should have affected its mechanical behavior.

Surprisingly, Figure 1(c) shows a high density of ⟨100⟩ edge and mixed dislocations, which is comparable to the density of ½⟨111⟩ edge and mixed dislocations. The perfect ⟨100⟩ dislocation is not common in coarse-grained bcc metals and is believed to be formed by the dislocation reaction: $\frac{1}{2}[111] + \frac{1}{2}[1\bar{1}\bar{1}] \rightarrow [100]$ [14]. This reaction is energetically favorable, but the magnitude of the ⟨100⟩ Burgers vector is ~15% larger than that of the ½⟨111⟩ Burgers vector, which makes the ⟨100⟩ dislocations less stable than the ½⟨111⟩ dislocations. The ⟨100⟩ dislocations are sessile dislocations. Since they are formed by the reaction of glissile ½⟨111⟩ dislocations, they can act to pin and stabilize ½⟨111⟩ dislocation networks in the grain interior, which explains why their density is comparable to that of the ½⟨111⟩ dislocations.

Figure 2 shows the effect of grain size on the density of screw dislocations. It clearly shows that the density of screw dislocations monotonically decreases with decreasing grain size from 500 to 100 nm. Significantly, the screw dislocations almost disappeared in grains smaller than 100 nm. Note that the screw dislocations cannot be identified in HRTEM micrographs.

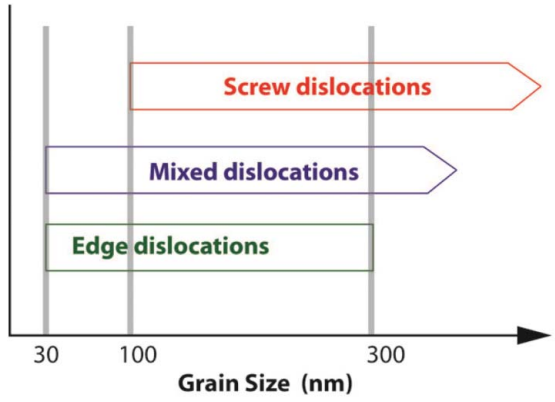

Figure 3. The range of grain sizes in which each type of dislocations was observed.

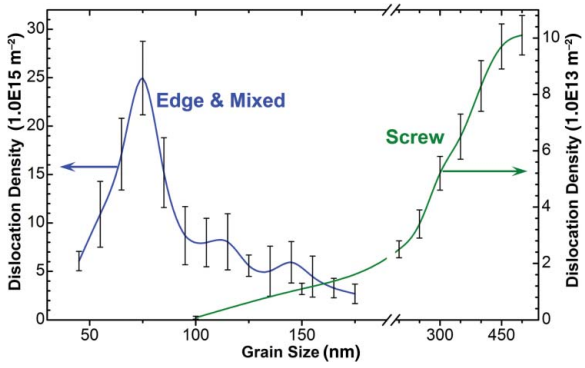

Figure 4. The variations of dislocation densities with grain size for ½⟨111⟩ screw dislocations and for ½⟨111⟩ edge and mixed dislocations. Note that the density of screw dislocations was measured using the $\vec{g} \cdot \vec{b}$ criterion, while the density of edge and mixed dislocations was measured from the HRTEM micrographs.

Instead, they are determined using the $\vec{g} \cdot \vec{b}$ criterion under two-beam conditions, where $\vec{g}$ and $\vec{b}$ are the diffraction vectors and the dislocation Burgers vector, respectively. The density of a screw dislocation is calculated as the total length of the screw dislocation segments per unit volume. More details on the measurement of screw dislocation density are given in the Supplementary Material.

The range of grain sizes in which each type of dislocations was observed is illustrated in Figure 3. As shown in the figure, screw dislocations were observed in grains larger than 100 nm, edge dislocations were observed in grains smaller than 300 nm and mixed dislocations exist in a broader range of grain sizes.

The density variations of ½⟨111⟩ screw dislocations and the density variation of ½⟨111⟩ edge and mixed dislocations are summarized in Figure 4. As shown in the figure, in grains with sizes larger than 300 nm, dislocations are mostly of screw type. Some mixed dislocations are also observed, but ½⟨111⟩ edge dislocations or ⟨100⟩ dislocations are difficult to find. The density of ½⟨111⟩ screw dislocations decreases monotonically with decreasing grain size and approaches zero when the grain size is below 100 nm. In contrast, the density of ½⟨111⟩ mixed and edge dislocations increases with decreasing grain size, reaches the maximum at the grain size of ~75 nm and then decreases when the grains become smaller. When the grain sizes are less than 30 nm, most grains are found to be dislocation free because of the annihilations of dislocations by grain boundaries.

Typical morphologies of various types of dislocations can be best observed using two-beam conditions to enhance their contrast. In Figure 5(a–c), the bright-field TEM micrographs taken from the [110] zone axis are shown, and in Figure 5(d–f), their corresponding micrographs taken under two-beam conditions using special diffraction vectors to image are shown. The two-beam condition images provide clearer images of dislocations. Figure 5(a) and (d) shows the segments of both edge and mixed dislocations in a 75-nm grain. Figure 5(b) and (e) shows the segments of a ½[111] edge dislocation (marked as E_{111}), a [100] edge dislocation (marked as E_{100}) and a ½[111] screw dislocation (marked as S_{111}) in a 140-nm grain. Figure 5(c) and (f) shows that the dislocations are mostly of screw type in a 300-nm grain. It appears that the dislocation segments become shorter in smaller grains. The procedure for the identification of the dislocation types is described in the Supplemental Material.

To understand the effect of grain size on the strain rate sensitivity in bcc metals and alloys, we need to first understand the deformation mechanism that controls the strain rate sensitivity. It is noted that the strain rate sensitivities of coarse-grained bcc metals are about an order of magnitude higher than that of the coarse-grained fcc metals [2,3,6,16–22]. This is caused by the difference in the dislocation core structures in fcc and bcc metals. A full dislocation may dissociate into partial dislocations to form a low-energy state. In fcc metals, both screw and edge dislocations may dissociate into two partials on a slip plane with a stacking fault between them [23,24]. These dislocations can easily glide on the slip plane with a relatively low strain rate sensitivity.

In contrast, in coarse-grained bcc metals, the mechanical behavior is controlled by the slip of the screw dislocations, especially in the early stage of deformation [2,6]. This is because a perfect screw dislocation ½[111] is believed to dissociate onto three different {110} slip planes or three different {112} slip planes [14,25]. Since the core of the ½[111] screw dislocation is spread onto three different slip planes, this makes it three dimensional (3D) and very hard to slip on any of the slip planes. Consequently, the slip of the screw dislocations in bcc metals is believed to proceed via side movements of edge dislocation kinks [26–29], which leads to a higher strain rate sensitivity in bcc metals. On the other hand, molecular

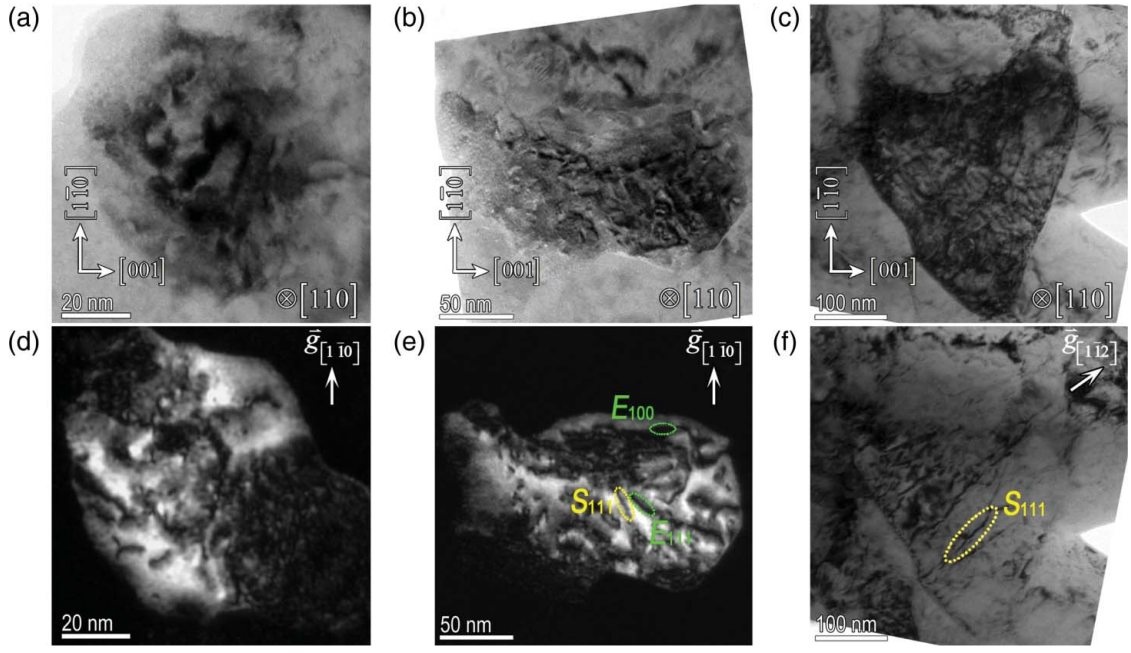

Figure 5. The variation of dislocation types in the grains with different sizes in HPT-processed Mo. (a–c) Bright-field TEM micrographs taken from the [110] zone axis and (d–f) their corresponding two-beam condition micrographs in which (d) and (e) are dark-field images using $\vec{g}_{[1\bar{1}0]}$ to image, while (f) is a bright-field image using $\vec{g}_{[1\bar{1}2]}$ to image. S_{111}, E_{111} and E_{100} denote the ½⟨111⟩ screw, ½⟨111⟩ and ⟨100⟩ edge dislocations, respectively.

dynamics simulations [30–33] revealed that the ½⟨111⟩ edge dislocations are very easy to glide, making it hard to retain them after deformation, which is why they are rarely observed experimentally in the postmortem observations under TEM. Therefore, the high strain rate sensitivity of the coarse-grained metals is caused by the movement of screw dislocations, which results in a very high strain rate sensitivity.

To understand how the dislocation types and their density affect the strain rate sensitivity, let us first invoke the relationship between strain rate and dislocation density and movement speed [34]:

$$\dot{\gamma} = b\rho v, \tag{2}$$

where $\dot{\gamma}$ is the shear strain rate and b is the magnitude of the Burgers vector of dislocations, which moves at the speed of v. The strain rate sensitivity m is defined as [2]

$$\frac{1}{m} = \frac{\partial \ln \dot{\gamma}}{\partial \ln \tau} = \frac{\partial \ln b\rho v}{\partial \ln \tau} = \frac{\partial \ln \rho v}{\partial \ln \tau}, \tag{3}$$

where τ is the shear stress.

In fcc metals and alloys, edge and screw dislocations glide at about the same speed and ρ is the total dislocation density. However, in bcc metals, edge dislocations move much faster than screw dislocations. For simplicity, we can qualitatively assume that the mixed dislocations behave like edge dislocations since the edge components of their Burgers vectors cannot dissociate into a 3D configuration like a screw dislocation. As will be discussed later, this assumption is reasonable for NC bcc metals. Following the above discussion, the strain rate of a bcc metal can be written as

$$\dot{\gamma} = b\rho_s v_s + b\rho_e v_e, \tag{4}$$

where ρ_s and v_s are the density and speed of screw dislocations, respectively, and ρ_e and v_e are the density and speed of dislocations with edge components (edge and mixed dislocations), respectively. From Equations (3) and (4), we can write

$$\frac{1}{m} = \frac{\partial \ln \dot{\gamma}}{\partial \ln \tau} = \frac{\partial \ln(\rho_s v_s + \rho_e v_e)}{\partial \ln \tau}. \tag{5}$$

In coarse-grained bcc metals where the deformation is primarily controlled by screw dislocations, $\rho_s v_s \gg \rho_e v_e$, Equation (5) can be approximated as

$$\frac{1}{m} \approx \frac{\partial \ln(\rho_s v_s)}{\partial \ln \tau} = \frac{1}{m_s}, \tag{6}$$

where m_s is the strain rate sensitivity caused by the screw dislocations, which is usually large as reported in coarse-grained bcc metals.

As illustrated in Figures 3 and 4, in NC bcc Mo, the density of screw dislocations ρ_s is close to zero. In addition, the screw dislocation moves much slower than the edge dislocations. Therefore, the deformation behavior of NC Mo is controlled by the gliding of edge dislocations.

Thus, Equation (5) can be approximated as

$$\frac{1}{m} \approx \frac{\partial \ln(\rho_e v_e)}{\partial \ln \tau} = \frac{1}{m_e}, \quad (7)$$

where m_e is the strain rate sensitivity caused by dislocations with edge components and is much lower than m_s. This explains why the NC bcc metals have a much lower strain rate sensitivity than their coarse-grained counterparts. It is interesting to note that the strain rate sensitivities of NC bcc metals are comparable to those of the coarse-grained fcc metals [6]. This is possibly because edge dislocations, which control the deformation behavior of NC bcc metals, move similar to how dislocations move in fcc metals, that is, gliding on slip planes easily. This observation also suggests that mixed dislocations, which have a high density in the NC bcc metals, produce a strain rate sensitivity similar to that produced by edge dislocations.

Therefore, the effect of grain size on the strain rate sensitivity in NC bcc metals is primarily caused by the change in deformation mechanisms. Coarse-grained bcc metals have a very high strain rate sensitivity because their deformations are controlled by the kink-pair-assisted movement of screw dislocations. NC bcc metals have a very low strain rate sensitivity because their deformation behavior is controlled by edge and mixed dislocations. The decrease in the strain rate sensitivity with decreasing grain size is caused by the decreasing density of screw dislocations and the increasing density of edge and mixed dislocations.

Our data also demonstrate that the dislocation density decreases with decreasing grain size when the grain sizes are smaller than 75 nm and few dislocations can be found in grains smaller than 30 nm. This suggests that grain boundary-mediated deformation processes such as grain boundary sliding, rotation and diffusion will play a more significant role with decreasing grain size in this range of grain sizes. Since a grain boundary-mediated process has a higher strain rate sensitivity, it may eventually lead to a higher strain rate sensitivity with decreasing grain size. Such a phenomenon is indeed observed in NC bcc metals [2,5,6].

In summary, we have observed a systematic change in the deformation mechanisms of NC bcc metals with grain size. As the grain size decreases, the density of screw dislocations approaches zero, while the density of dislocations with edge components increases, leading to a decrease in the strain rate sensitivity. The deformation behavior is eventually controlled by dislocations with edge components, and this produces the lowest strain rate sensitivity. Further decreasing grain sizes resulted in the decrease in all dislocations, and grain boundary-mediated processes start to play a more significant role, leading to a slight increase in the strain rate sensitivity.

Supplementary online material. A more detailed information on experiments is available at http://dx.doi.org/10.1080/21663831.2012.739580.

Acknowledgements This work was supported by the Laboratory Directed Research and Development program office of the Idaho National Laboratory. The authors thank Dr Dieter Wolf, whose insight and discussions with the authors inspired and initiated the current study on bcc metals.

References

[1] Malow TR, Koch CC. Mechanical properties, ductility, and grain size of nanocrystalline iron produced by mechanical attrition. Metallurgical and Materials Transactions A. 1998;29(9):2285–95.
[2] Wei Q, Cheng S, Ramesh KT, Ma E. Effect of nanocrystalline and ultrafine grain sizes on the strain rate sensitivity and activation volume: fcc versus bcc metals. Materials Science and Engineering A. 2004;381(1–2):71–9.
[3] Jia D, Ramesh KT, Ma E. Effects of nanocrystalline and ultrafine grain sizes on constitutive behavior and shear bands in iron. Acta Materialia. 2003;51(12):3495–509.
[4] Wei Q, Jiao T, Ramesh KT, Ma E, Kecskes LJ, Magness L, Dowding R, Kazykhanov VU, Valiev RZ. Mechanical behavior and dynamic failure of high-strength ultrafine grained tungsten under uniaxial compression. Acta Materialia. 2006;54(1):77–87.
[5] Wei Q, Pan ZL, Wu XL, Schuster BE, Kecskes LJ, Valiev RZ. Microstructure and mechanical properties at different length scales and strain rates of nanocrystalline tantalum produced by high-pressure torsion. Acta Materialia. 2011;59(6):2423–36.
[6] Wei Q. Strain rate effects in the ultrafine grain and nanocrystalline regimes-influence on some constitutive responses. The Journal of Materials Science. 2007;42(5):1709–27.
[7] Wasserbach W. Development of the dislocation arrangement in high-purity Nb-34at-percent-Ta alloy single-crystals deformed in tension. Physica Status Solidi A. 1995;151(1):61–82.
[8] Les P, Stuewe HP, Zehetbauer M. Hardening and strain rate sensitivity in stage IV of deformation in fcc and bcc metals. Materials Science and Engineering A. 1997;234(1):453–5.
[9] Jiang HG, Zhu YT, Butt DP, Alexandrov IV, Lowe TC. Microstructural evolution, microhardness and thermal stability of HPT-processed Cu. Materials Science and Engineering A. 2000;290(1):128–38.
[10] Zhilyaev AP, Langdon TG. Using high-pressure torsion for metal processing: fundamentals and applications. Progress in Materials Science. 2008;53(6):893–979.
[11] Zhu YT, Huang JY, Gubicza J, Ungar T, Wang YM, Ma E, Valiev RZ. Nanostructures in Ti processed by severe plastic deformation. Journal of Materials Research. 2003;18(8):1908–17.
[12] Huang JY, Zhu YT, Jiang H, Lowe TC. Microstructures and dislocation configurations in nanostructured Cu processed by repetitive corrugation and straightening. Acta Materialia. 2001;49(9):1497–505.
[13] Balogh L, Ungar T, Zhao Y, Zhu YT, Horita Z, Xu C, Langdon TG. Influence of stacking-fault energy on microstructural characteristics of ultrafine-grain copper and copper-zinc alloys. Acta Materialia. 2008;56(4):809–20.

[14] Hirth JP, Lothe J. Theory of dislocations. 2nd ed. Malabar, FL: Krieger Publishing Company; 1992.
[15] Nabarro FRN. Dislocations in solids. Oxford: North-Holland Press; 1979.
[16] Chen J, Lu L, Lu K. Hardness and strain rate sensitivity of nanocrystalline Cu. Scripta Materialia. 2006;54(11):1913–8.
[17] Carreker RP, Hibbard WR. Tensile deformation of high-purity copper as a function of temperature, strain rate, and grain size. Acta Metallurgica. 1953;1(6):654–63.
[18] Dalla Torre FH, Pereloma EV, Davies CHJ. Strain hardening behaviour and deformation kinetics of Cu deformed by equal channel angular extrusion from 1 to 16 passes. Acta Materialia. 2006;54(4):1135–46.
[19] Wei Q, Jiao T, Mathaudhu SN, Ma E, Hartwig KT, Ramesh KT. Microstructure and mechanical properties of tantalum after equal channel angular extrusion (ECAE). Materials Science and Engineering A. 2003;358(1–2):266–72.
[20] Wei Q, Kecskes L, Jiao T, Hartwig KT, Ramesh KT, Ma E. Adiabatic shear banding in ultrafine-grained Fe processed by severe plastic deformation. Acta Materialia. 2004;52(7):1859–69.
[21] Wei Q, Ramesh KT, Ma E, Kesckes LJ, Dowding RJ, Kazykhanov VU, Valiev RZ. Plastic flow localization in bulk-tungsten with ultrafine microstructure. Applied Physics Letters. 2005;86(10):101907.
[22] Wei Q, Jiao T, Ramesh KT, Ma E. Nano-structured vanadium: processing and mechanical properties under quasi-static and dynamic compression. Scripta Materialia. 2004;50(3):359–64.
[23] Zhu YT, Liao XZ, Wu XL. Deformation twinning in nanocrystalline materials. Progress in Materials Science. 2012;57(1):1–62.
[24] Liao XZ, Srinivasan SG, Zhao YH, Baskes MI, Zhu YT, Zhou F, Lavernia EJ, Xu HF. Formation mechanism of wide stacking faults in nanocrystalline Al. Applied Physics Letters. 2004;84(18):3564–6.
[25] Amelinckx S. Dislocations in particular structures. New York: North-Holland Publishing Company; 1979.
[26] Dorn JE, Rajnak S. Nucleation of Kink Pairs + Peierls mechanism of plastic deformation. Transactions of the Metallurgical Society of the American Institute of Mechanical Engineers. 1964;230(5):1052–64.
[27] Tang M, Kubin LP, Canova GR. Dislocation mobility and the mechanical response of BCC single crystals: a mesoscopic approach. Acta Materialia. 1998;46(9): 3221–35.
[28] Stainier L, Cuitino AM, Ortiz M. A micromechanical model of hardening, rate sensitivity and thermal softening in bcc single crystals. Journal of the Mechanics and Physics of Solids. 2002;50(7):1511–45.
[29] Chang JP, Bulatov VV, Yip S. Molecular dynamics study of edge dislocation motion in a bcc metal. Journal of Computer-Aided Materials Design. 1999;6(2–3):165–73.
[30] Liu RP, Wang SF, Wang R, Jiao JA. The theoretical investigations of the core structure and the Peierls stress of the $1/2\langle 111\rangle\{110\}$ edge dislocation in Mo. Materials Science and Engineering A. 2010;527(18–19):4887–90.
[31] Liu XL, Golubov SI, Woo CH, Huang HC. Glide of edge dislocations in tungsten and molybdenum. Materials Science and Engineering A. 2004;365(1–2):96–100.
[32] Monnet G, Terentyev D. Structure and mobility of the $1/2\langle 111\rangle\{112\}$ edge dislocation in BCC iron studied by molecular dynamics. Acta Materialia. 2009;57(5):1416–26.
[33] Duesbery MS, Xu W. The motion of edge dislocations in body-centered cubic metals. Scripta Materialia. 1998;39(3):283–7.
[34] Orowan E. Problems of plastic gliding. Proceedings of the Physical Society. 1940;52(1):8–22.